JOURNAL OF AIRCRAFT
Vol. 42, No. 2, March–April 2005

Application of Genetic Algorithm for Aeroelastic Tailoring of a Cranked-Arrow Wing

Hitoshi Arizono*
Japan Aerospace Exploration Agency, Tokyo 181-0015, Japan
and
Koji Isogai†
Nippon Bunri University, Oita 870-0397, Japan

A computer code for aeroelastic tailoring of a cranked-arrow wing for a supersonic transport is developed. The code includes static strength, local buckling, and aeroelastic analyses. The original finite element code is used for the static strength and local buckling analyses, and the original code is used for the vibration analysis of the aeroelastic analysis. In the optimization process of this code, a genetic algorithm is employed to find the optimum laminate construction of the wing box for which the structural weight is minimum under the static strength, local buckling, and aeroelastic constraints. These codes are applied to the preliminary design of a cranked-arrow wing. The optimum design satisfying only the static strength and local buckling constraints does not satisfy the aeroelastic constraint. Therefore, the flutter characteristics are optimized, and the optimum laminate construction that satisfies the static strength, local buckling, and aeroelastic constraints is obtained.

Introduction

SINCE the end of the 1980s, research and development into the next-generation supersonic transport (SST) has been active throughout the world in order to satisfy passenger demand for high-speed transportation. The cranked-arrow wing might be a strong candidate for the main wing of a SST. Aeroelastic characteristics are significant with respect to the structural design of a cranked-arrow wing intended for use in the transonic regime.[1] For example, design studies by Turner and Grande[2] on the early Boeing Supersonic Transport Model 969-512B revealed that the strength-designed configuration did not meet the flutter requirement, and an unrealistically high mass penalty was expected in order to clear the flutter requirement ($1.2V_D = 259$ m/s EAS at $M = 0.9$) in the initial design.

To improve the flutter characteristics of a cranked-arrow wing without a resulting mass penalty, the application of aeroelastic tailoring technology[3] might be one of the most promising approaches. Aeroelastic tailoring is the concept whereby directional stiffness is actively employed in the structural design of the aircraft in order to control the static or dynamic characteristics. However, the effectiveness of the aeroelastic tailoring of the cranked-arrow wing has not been examined thoroughly, although this technique has been shown to be highly effective with respect to the high-aspect-ratio transport-type wing.[4]

Currently, software such as TSO,[5] FASTOP,[6] and ASTROS[7] has been developed for use in aeroelastic tailoring. However, the software just mentioned requires knowledge of the derivatives of the flutter velocity with respect to each design variable in the optimization processes. In TSO, although the fiber orientation angles of composites can be treated as design variables, the finite element method is not employed in the structural analysis, whereas in FASTOP and ASTROS the fiber orientation angles cannot be treated as design variables.

Received 25 December 2002; revision received 3 August 2004; accepted for publication 13 August 2004.

*Researcher, Structural Research Group, Institute of Space Technology and Aeronautics, 6-13-1 Osawa, Mitaka; arizono.hitoshi@jaxa.jp. Member AIAA.

†Professor, Department of Aeronautics and Astronautics, 1727 Ichigi; isogai@nbu.ac.jp. Associate Fellow AIAA.

The genetic algorithm (GA) was developed by Holland[8] and is based on the evolutionary process and Darwin's concept of natural selection. Genetic algorithms do not depend on the derivatives of the objective and constraint functions. In addition, GAs are robust, making them suitable to multiple-peak problems.

We have developed a computer code for aeroelastic tailoring using a genetic algorithm in the optimization procedure. The present paper describes the results obtained by applying this newly developed code to a cranked-arrow wing.

Description of the Computer Code

Conventional airplanes use a wing-box structure, which includes the skin panels, spars, and ribs. In aeroelastic tailoring, the design variables include those associated with composite construction, such as the thicknesses and fiber orientation angles of the skin panels. Composite construction of skin panels can be used to vary the static and dynamic characteristics of the wing and thus to control the aeroelastic characteristics.

A flowchart of the computer code for aeroelastic tailoring is shown in Fig. 1. This computer code consists of four major parts: static strength analysis, local buckling analysis, aeroelastic analysis, and an optimization process. All code was developed in house. In the static strength analysis, the strains computed via the finite element method[9] (FEM) are examined under a prescribed load. This steady aerodynamic load is computed using the doublet-lattice method[10] (DLM). In the local buckling analysis, the buckling loads of the areas enclosed by spars and ribs are investigated. In addition, the in-plane loads of these areas, which are constrained under the prescribed load, are also investigated. The buckling loads and the in-plane loads are computed via FEM. In the aeroelastic analysis, the flutter velocity and the flutter frequency are computed using the $U - g$ method. The natural frequencies and natural vibration modes needed for use in the $U - g$ method are computed via FEM. The unsteady aerodynamic force is computed using DLM. In the optimization process, a genetic algorithm is used. In the laminated composite structure, each lamina has its greatest stiffness and strength properties along the direction in which the fibers are oriented. Therefore, the mechanical properties of laminated composite structures depend largely on laminate construction. Laminate construction considers design variables such as ply thickness and orientation and can result in discontinuous behavior of the objective function. The GA is an ideal optimization method, having no requirement for the derivatives of the objective or constraint functions.

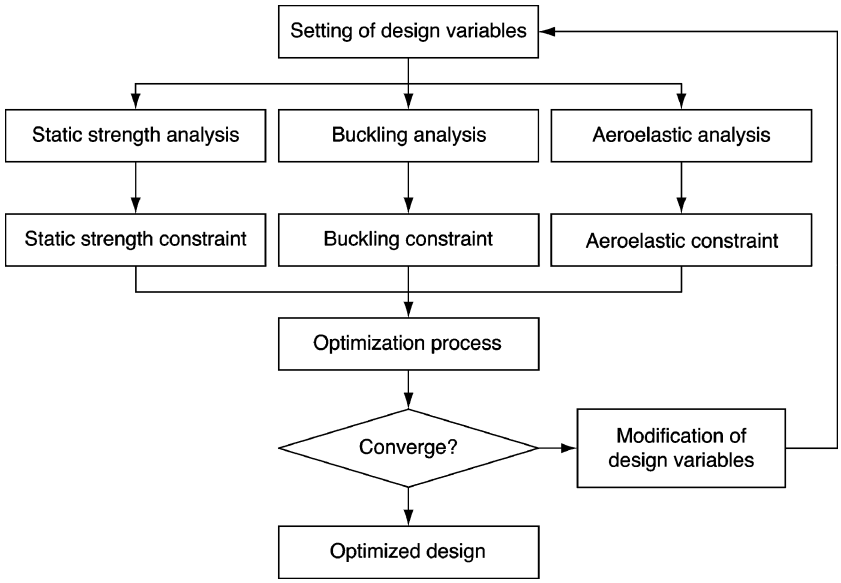

Fig. 1 Flowchart of aeroelastic tailoring.

Table 1 Natural frequencies of the theoretical and analytical analyses

Mode	Theory, Hz	FEM, Hz	Error, %
1	3.46	3.50	1.0
2	21.72	21.46	−1.2
3	60.81	58.10	−4.5
4	119.12	119.41	0.2

Verification of the Code

Verification of the buckling analysis code is performed using the model shown in Fig. 2. In this model, all sides are simply supported, and compressive loads are imposed in the x direction. For comparison with the theoretical buckling load,[11] the length of side b is 1.0 m and the length of side a is varied from 0.1 to 6.0 m. The plate thickness is 0.001 m. The FEM model is divided into 10×10 elements and is triangulated. Figure 3 compares the theoretical buckling load and the buckling load obtained analytically using the FEM code. The error is approximately 2 to 5%. In the case of $a/b \geq 2$, the error is higher because the triangles become longer and more narrow as a/b becomes larger. However, in this study the maximum value of a/b is approximately 4.5. Thus, the buckling analysis code used herein gives reasonable results.

Verification of the vibration analysis code is performed using the model as shown in Fig. 4. This model is a simple cantilevered box beam. In this model, $a = 20$ m, $b = 1.0$ m, $c = 0.5$ m, $b_1 = 0.005$ m, and $c_1 = 0.001$ m. The material properties are $E = 207$ GPa, $\nu = 0.3$, and $\rho = 7861$ kg/m^3. The theoretical[12] and FEM-based analytical results for the natural frequencies are listed in Table 1. Although isotropic materials are employed, reasonable results are obtained by changing the stiffness matrix appropriately.

Vehicle Configuration

The cranked-arrow wing employed in the present study is shown in Fig. 5. This model is based on the Boeing Supersonic Transport Model 969-512B (Ref. 2). The root chord is 50.4 m, and the semispan length is 18.9 m. The full-span wing area is 821.4 m^2, and the aspect ratio is 1.74. The airfoil section is a symmetric circular arc, and the airfoil thickness is 3%. The wing box is a multispar box structure. The engine masses are assumed to be 6500 kg for each engine and are set as concentrated masses centered at the locations indicated in Fig. 5. For the full fuel condition, which is the most critical condition for flutter, the fuel mass is assumed to be 200,000 kg. In addition, the fuel mass is assumed to be loaded in the space of the box structure. The mass of the fuel is distributed

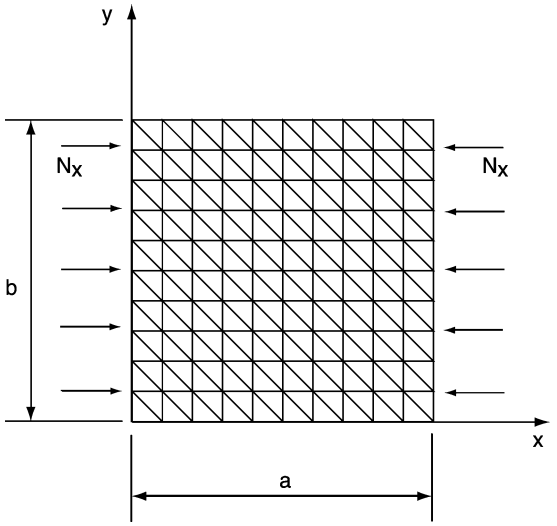

Fig. 2 Model used to verify the buckling analysis code.

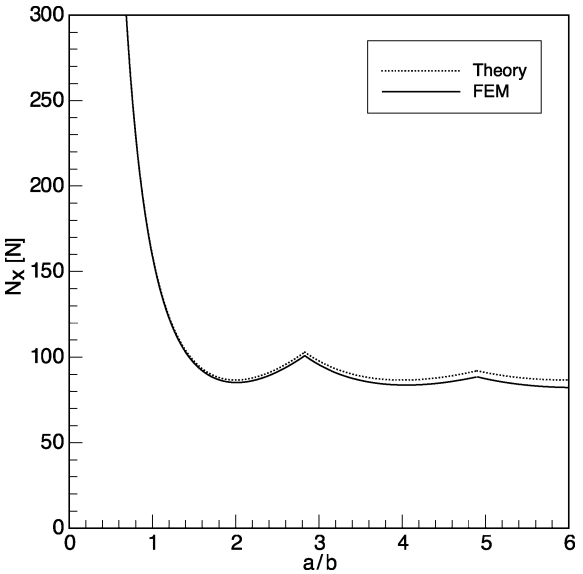

Fig. 3 Theoretical and analytical buckling loads.

according to density on the elements of the upper and lower skin panels.

Analytical Model

Figure 6 shows the FEM model, which consists of 680 nodes and 2008 triangular elements. In the static strength and vibration analyses, the elements are the membrane elements, and in the local buckling analysis the elements are the plate bending elements. The boundary conditions are follows: in the static strength analysis the wing root is assumed to be fixed, in the local buckling analysis the area enclosed by spars and ribs is assumed to be a simply supported plate, in the vibration analysis displacements in the x and z directions and pitching movements of the root are permitted in the symmetric mode, and displacement in the y direction and rolling and yawing movements are permitted in the antisymmetric mode.

The properties of the heat resisting composite materials are $E_1 = 157$ GPa, $E_2 = 9.8$ GPa, $\nu = 0.34$, $G_{12} = 4.9$ GPa, and $\rho = 1600$ kg/m^3.

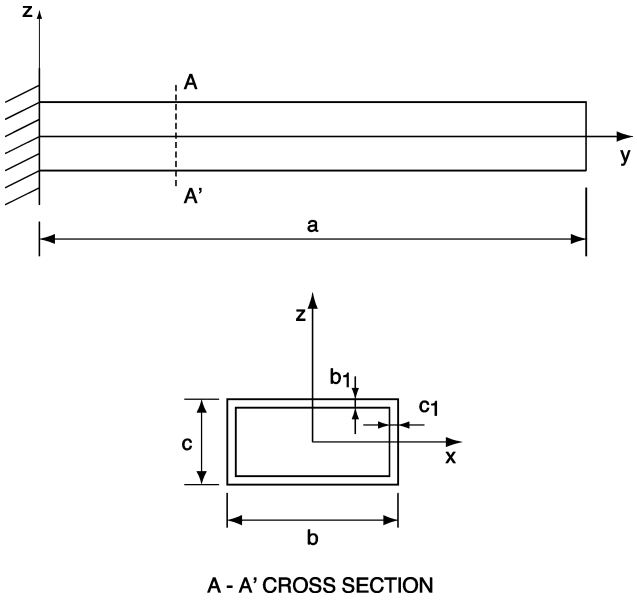

Fig. 4 Model used to verify the vibration analysis code.

Design Variables

To investigate the effect of the fiber orientation angles, the laminate construction of the upper and lower skin panels is assumed to be $[0_1 \text{ deg}/+45_1 \text{ deg}/90_1 \text{ deg}/-45_1 \text{ deg}]_s$ for model A and $[\alpha_1/\beta_1]_s$ for model B. Here, α and β are the different fiber orientation angles and are used as design variables, as shown in Fig. 7. The subscript s denotes a symmetric layup. In terms of the spars and ribs, the laminate construction is assumed to be quasi-isotropic $[0_1 \text{ deg}/+45_1 \text{ deg}/90_1 \text{ deg}/-45_1 \text{ deg}]_s$.

To avoid an unrealistic thickness distribution and reduce the number of design variables in the optimization process, in which each element of the FEM model is a design variable, the upper and lower skin panels are each divided into six zones, as shown in Fig. 7. The zones of the spars and ribs are shown in Fig. 8. The thickness of each zone is assumed to be constant.

Therefore, the design variables are as follows: 1) fiber orientation angle of the upper and lower skin panels (2:α, β), 2) thickness of the upper skin panels of each zone (6:skin I $\sim$ VI), 3) thickness of the lower skin panels of each zone (6:skin VII $\sim$ XII), 4) thickness of the fore-spars (1:spar I), 5) thickness of the hind-spars (1:spar II), and 6) thickness of each rib (6:rib I $\sim$ rib VI). The total number of design variables is 20 for model A and 22 for model B. The ranges of the fiber orientation angles α and β are -90 deg to $+90$ deg. The minimum gauge for the upper and lower skin panels, spars, and ribs is assumed to be 1.92 mm.

Optimization Procedure

Aeroelastic tailoring for the cranked-arrow wing shown in Fig. 5 involves the optimization procedure described next.

The objective function is the structural weight of the wing box, namely, the sum of the weights of the upper and lower skin panels, spars, and ribs.

The static strength constraint is a sustained 2.5-g load at maximum takeoff gross weight, which is 9.186×10^6 N. The static load can be maintained for a Mach number of 0.9 and an angle of attack of 5.2 deg. Figure 9 shows the load distributions predicted using the DLM, in which 100 panels (10 chordwise by 10 spanwise) are employed. The maximum strain criterion[11] is employed to identify structural failure. The structural constraint should satisfy the following equation:

$$X_c < \epsilon_1 < X_t, \qquad Y_c < \epsilon_2 < Y_t, \qquad |\gamma_{12}| < S_\epsilon \tag{1}$$

where ϵ_1, ϵ_2, and γ_{12} are the strain for a 2.5-g load, X_t and X_c are the maximum tensile and compressive normal strains in the 1 direction,

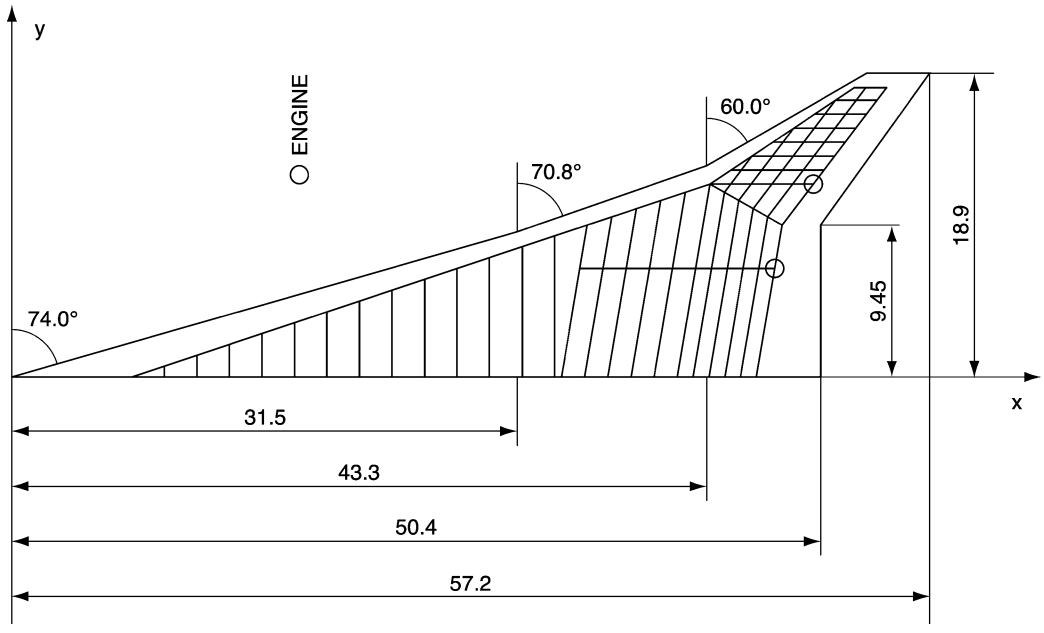

Fig. 5 Cranked-arrow wing.

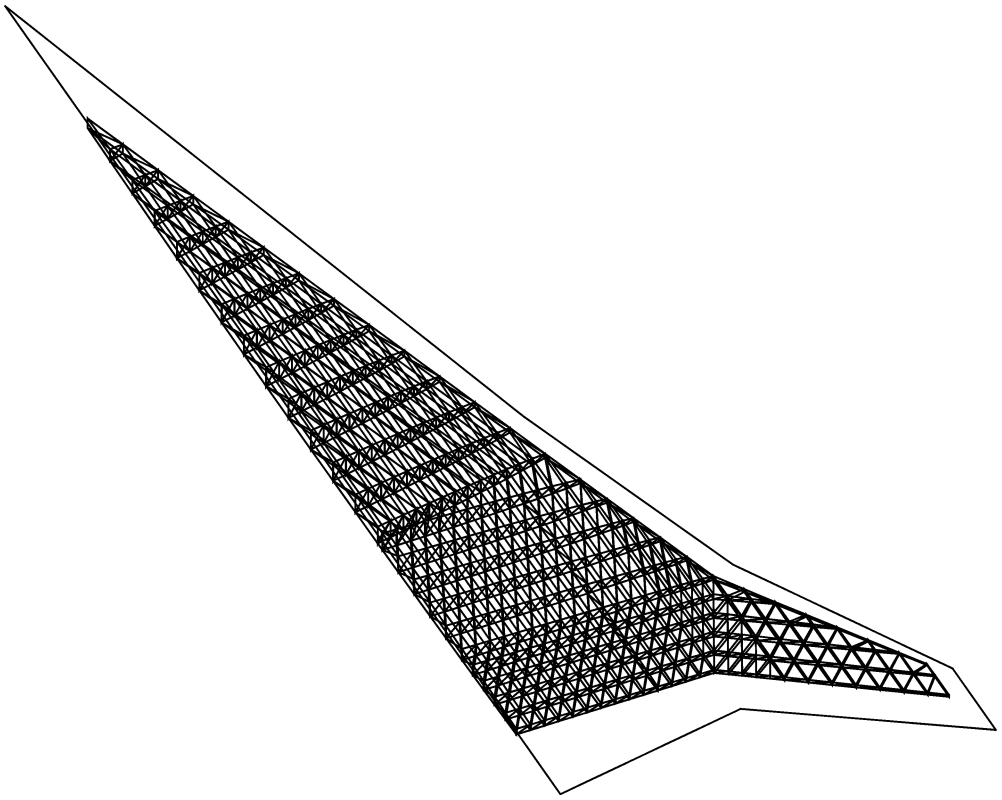

Fig. 6 Finite element model.

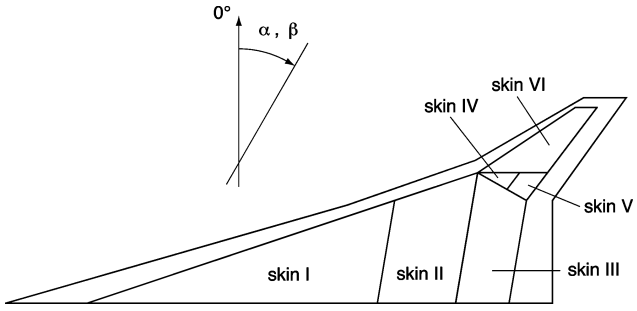

Fig. 7 Zones of upper and lower skin panels.

Y_t and Y_c are the maximum tensile and compressive normal strains in the 2 direction, and S_ϵ is the maximum shear strain in the 1–2 plane. In this study, the following relationships hold: $X_t = Y_t = 4000\mu$, $X_c = Y_c = -4000\mu$, and $S_\epsilon = 8000\mu$.

The local buckling constraint is to satisfy the following equation:

$$N_x/N_{x\mathrm{cr}} + N_y/N_{y\mathrm{cr}} + (N_{xy}/N_{xy\mathrm{cr}})^2 < 1 \qquad (2)$$

where N_x, N_y, and N_{xy} are the in-plane loads, and $N_{x\mathrm{cr}}$, $N_{y\mathrm{cr}}$, and $N_{xy\mathrm{cr}}$ are the buckling loads. These loads are computed with respect to each area enclosed by spars and ribs.

For the aeroelastic analysis, the symmetric/antisymmetric natural vibration modes are 10 mode shapes, including the rigid-body modes. For the aeroelastic constraint, the symmetric/antisymmetric flutter velocities must be higher than $1.2V_D = 259$ m/s EAS (where V_D is the design diving speed) at $M = 0.9$. The structural damping is zero in this study.

Figure 10 shows the flowchart of the optimization process using the genetic algorithm. For the implementation of the genetic algorithm in the optimization process, an initial population of the binary coding of design variables with randomly chosen genes is created. The size of the population used in the present code is 40 and remains constant throughout the genetic optimization. The fitness function is the inverse of the structural weight. If the individual does not satisfy the constraints, the structural weight is increased by a factor of 10, which reduces the fitness value. The method of selection is tournament selection,[13] in which two individuals are chosen at random from the population and the individual with the higher fitness value is selected to be a parent. These two individuals are then returned to the original population and selection is performed again. In elitism,[14] the best individual is passed on to the next generation. The advantage of elitism is that the best individual is not lost if it is not selected for reproduction or if it is destroyed by crossover or mutation. The method of crossover used herein is one-point crossover, in which children are created by combining a portion of each parent's genetic string in an operation. The probability of crossover is 0.6. In mutation, a single gene is selected randomly, and its bit is inverted. The probability of mutation is 0.02.

Table 2 Structural weights for models A1, A2, and A3 (inkg)

Parameter	Model A1	Model A2	Model A3
Skin panels	5557	6019	6737
Spars	2224	1436	1673
Ribs	889	1474	756
Total	8670	8929	9166

Numerical Results

Optimum Design of Quasi-Isotropic Laminates

The computations are conducted under three conditions: only the static strength constraint is satisfied (model A1); both the static strength and local buckling constraints are satisfied (model A2); and the static strength, local buckling, and aeroelastic constraints are satisfied (model A3).

Figure 11 shows the convergence histories of the structural weights for models A1, A2, and A3. The total structural weight of the wing box for the semispan wing in optimum laminate construction is 8670 kg for model A1, 8929 kg for model A2, and 9166 kg for model A3. Table 2 lists the structural weights of skin

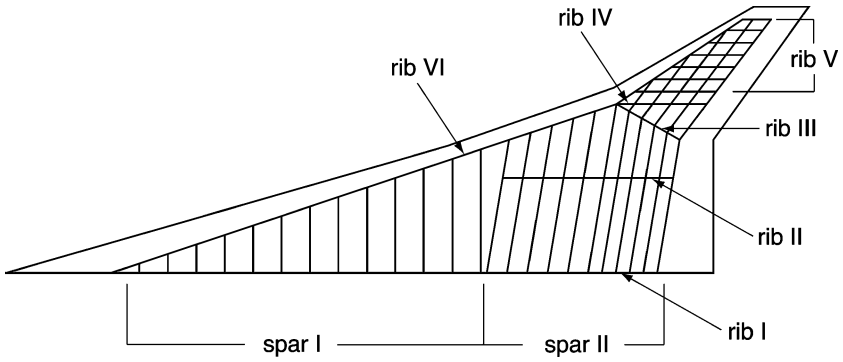

Fig. 8 Zones of spars and ribs.

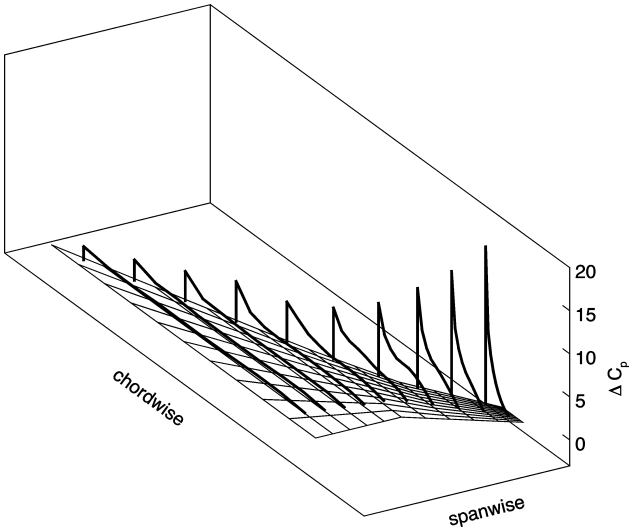

Fig. 9 Load distribution.

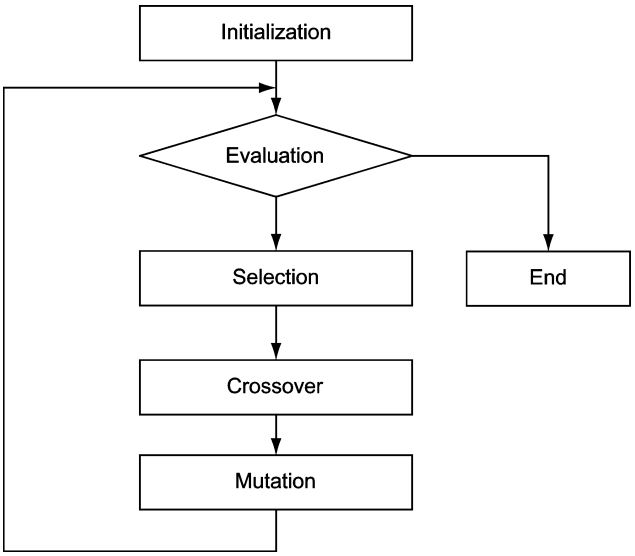

Fig. 10 Flowchart of the genetic algorithm.

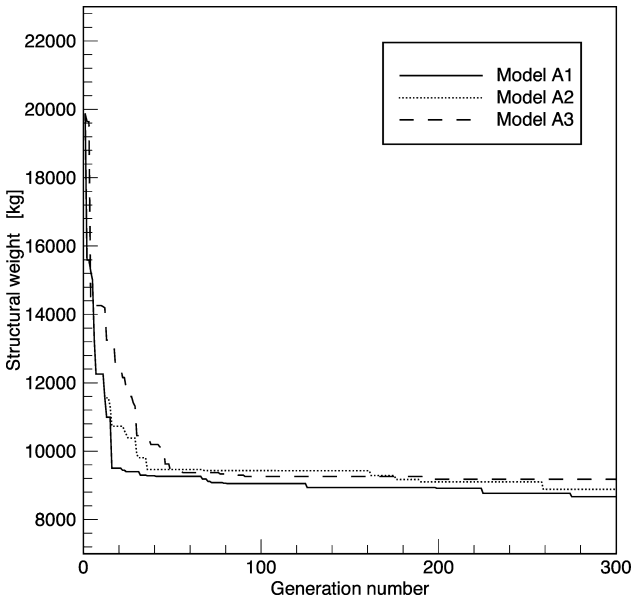

Fig. 11 Convergence histories of structural weights of models A1, A2, and A3.

panels, spars, and ribs. The optimum design of the thickness distributions is obtained from the individual having the best fitness in the 300th generation. The weight of spars in model A1 is somewhat larger than in the other models. In particular, the weight of web II is larger in model A1. This seems to be because the bending stiffness is increased in order to satisfy the static strength constraint.

Figure 12 shows the thickness distributions of the upper and lower skin panels for models A1, A2, and A3. The thicknesses of the upper and lower skin panels are seen generally to increase from model A1 to A3. As just mentioned, the increase in stiffness results in the satisfaction of the aeroelastic constraint.

The flutter speeds and frequencies for models A1, A2, and A3 are listed in Table 3. Models A1 and A2 do not satisfy the aeroelastic constraint. However, by optimizing the flutter characteristics an optimum design that satisfies all of the constraints is finally achieved.

Optimum Design of Laminate Construction

The fiber orientation angles of the upper and lower skin panels are added to the design variables in order to increase the flexibility of the design. As in the previous computations, the computations are conducted under three conditions: only the static strength constraint is satisfied (model B1); both the static strength and local buckling constraints are satisfied (model B2); and the static strength, local buckling, and aeroelastic constraints are satisfied (model B3).

Figure 13 shows the convergence histories of the structural weights for models B1, B2, and B3. The total structural weight of the wing box for the semispan wing in the optimum laminate construction is 7894 kg for model B1, 8418 kg for model B2, and 8578 kg for model B3. Table 4 lists the structural weights of skin panels, spars, and ribs. The optimum design of the fiber orientation angles and the thickness distributions is obtained from the individual having the best fitness in the 300th generation. The structural weight of model B3 is lighter than that of model A3 by approximately 6.4% because in model B3 the fiber orientation angles are added to the design variables. Thus, compared with the optimum design using

Table 3 Flutter speeds and frequencies for models A1, A2, and A3

Parameter	Model A1	Model A2	Model A3
Symmetric mode			
Flutter speed, m/s	679.2	775.8	785.0
Flutter frequency, rad/s	23.7	25.3	38.9
Antisymmetric mode			
Flutter speed, m/s	152.0	144.2	353.9
Flutter frequency, rad/s	22.7	25.7	46.9

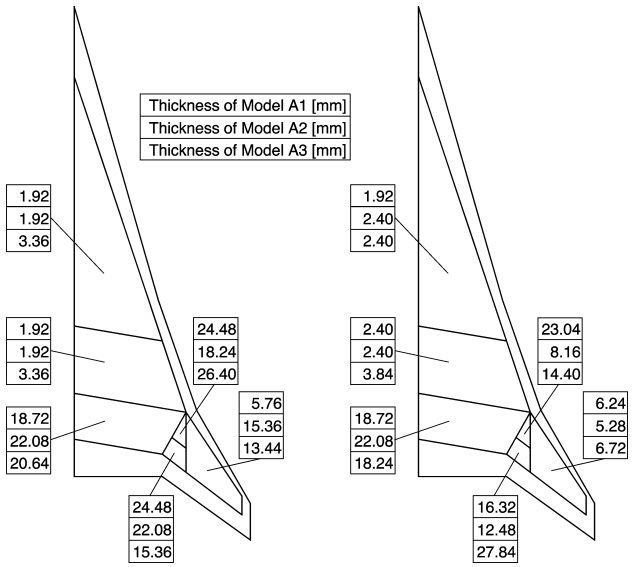

a) Upper skin panel **b) Lower skin panel**

Fig. 12 Thickness distributions of the upper and lower skin panels of models A1, A2, and A3.

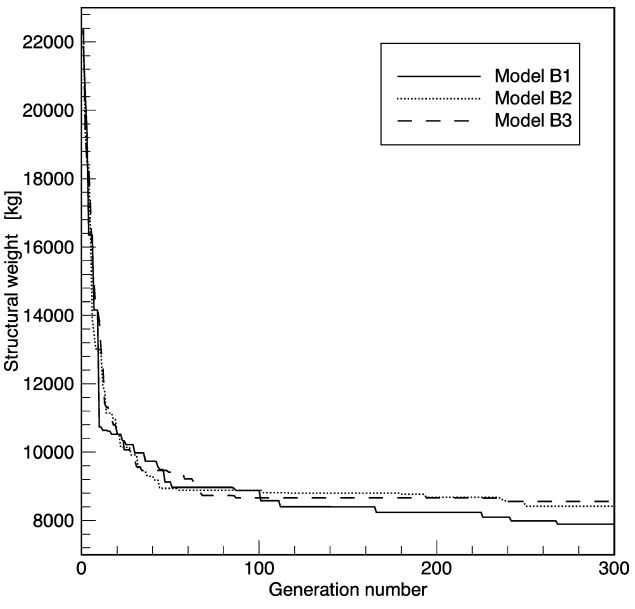

Fig. 13 Convergence histories of structural weights of models B1, B2, and B3.

quasi-isotropic laminates, a further reduction in structural weight is possible for model B3.

Figure 14 shows the fiber orientation angles and the thickness distributions of the upper and lower skin panels for models B1, B2, and B3. The increase in the thicknesses of the outboard skin panels is remarkable, and the thicknesses of the hind-inboard skin panels can be seen to decrease. These tendencies indicate that torsional stiffness increases toward the wing tip and bending stiffness decreases towards the wing root in order to satisfy the aeroelastic constraint.

Table 4 Structural weights for models B1, B2, and B3 (inkg)

Parameter	Model B1	Model B2	Model B3
Skin panels	4087	4406	4513
Spars	2851	2745	2852
Ribs	956	1267	1213
Total	7894	8418	8578

Table 5 Flutter speeds and frequencies for models B1, B2, and B3

Parameter	Model B1	Model B2	Model B3
Symmetric mode			
Flutter speed, m/s	654.5	527.4	372.3
Flutter frequency, rad/s	22.8	31.1	30.3
Antisymmetric mode			
Flutter speed, m/s	246.0	182.7	567.1
Flutter frequency, rad/s	23.5	24.5	34.6

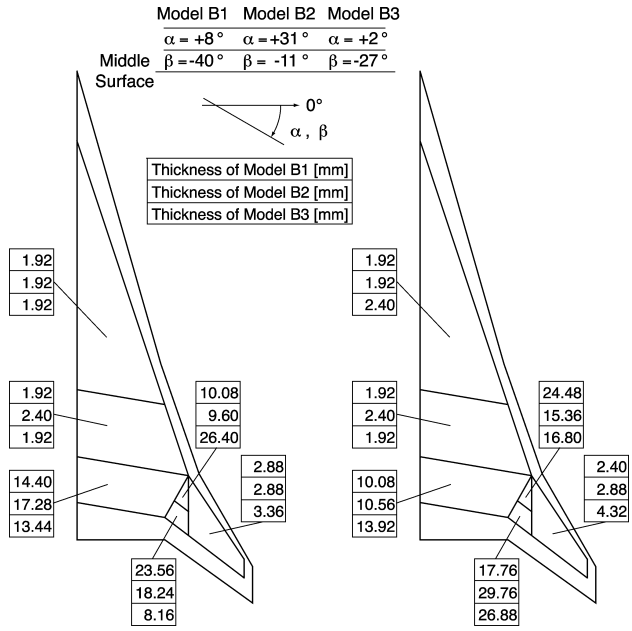

a) Upper skin panel **b) Lower skin panel**

Fig. 14 Thickness distributions of the upper and lower skin panels of models B1, B2, and B3.

The flutter speeds and frequencies for models B1, B2, and B3 are listed in Table 5. Like models A1 and A2, models B1 and B2 do not satisfy the aeroelastic constraint.

Conclusions

A computer code for aeroelastic tailoring of a cranked-arrow wing for a supersonic transport was developed. The newly developed code includes static strength and local buckling analyses using the original finite element code and aeroelastic analysis. In the optimization process of this code, a genetic algorithm is employed in order to determine the optimum laminate construction of the wing box for the minimum structural weight under the static strength, local buckling, and aeroelastic constraints. The newly developed code is applied to the preliminary design of a cranked-arrow wing.

Neither the optimum design satisfying only the static strength constraint nor that satisfying both the static strength and the local buckling constraints satisfies the aeroelastic constraint. Therefore, the flutter characteristics are optimized, and the optimum laminate construction that satisfies the static strength, local buckling, and aeroelastic constraints is obtained.

References

[1]Bhatia, K. G., and Wertheimer, J., "Aeroelastic Challenges for a High Speed Civil Transport," AIAA Paper 93-1478, April 1993.

[2]Turner, M. J., and Grande, D. L., "Study of Advanced Composite Structural Design Concepts for an Arrow Wing Super Sonic Cruise Configuration," NASA CR 2825, April 1978.

[3]Shirk, M. H., Hertz, T. J., and Weisshaar, T. A., "Aeroelastic Tailoring—Theory, Practice and Promise," *Journal of Aircraft*, Vol. 23, No. 1, 1986, pp. 6–18.

[4]Isogai, K., "Direct Search Method to Aeroelastic Tailoring of a Composite Wing Under Multiple Constraints," *Journal of Aircraft*, Vol. 26, No. 12, 1989, pp. 1076–1080.

[5]McCullers, L. A., and Lynch, R. W., "Dynamic Characteristics of Advanced Filamentary Composite Structures, Volume II—Aeroelastic Synthesis Procedure Development," AFFDL-TR-73-111, Sept. 1974.

[6]Wilkinson, K., Markowitz, J., Lerner, E., George, D., and Batill, S. M., "FASTOP: A Flutter and Strength Optimization Program for Lifting-Surface Structures," *Journal of Aircraft*, Vol. 14, No. 6, 1977, pp. 581–587.

[7]Neill, D. J., Johnson, E. H., and Canfield, R., "ASTROS—A Multidisciplinary Automated Structural Design Tool," *Journal of Aircraft*, Vol. 27, No. 12, 1990, pp. 1021–1027.

[8]Holland, J. H., *Adaptation in Natural and Artificial Systems: an Introductory Analysis with Applications to Biology, Control, and Artificial Intelligence*, MIT Press, Cambridge, MA, 1992.

[9]Zienkiewicz, O. C., and Taylor, R. L., *The Finite Element Method*, Vols. 1 and 2, 5th ed., Butterworth-Heinemann, Woburn, MA, 2000.

[10]Albano, E., and Rodden, W. P., "A Doublet-Lattice Method for Calculating Lift Distributions on Oscillating Surfaces in Subsonic Flows," *AIAA Journal*, Vol. 7, No. 2, 1969, pp. 279–285.

[11]Jones, R. M., *Mechanics of Composite Materials*, 2nd ed., Taylor and Francis, Philadelphia, 1999.

[12]Blevins, R. D., *Formulas for Natural Frequency and Mode Shape*, Van Nostrand Reinhold, 1979.

[13]Goldberg, D. E., "A Note on Boltzmann Tournament Selection for Genetic Algorithms and Population-Oriented Simulated Annealing," *Complex Systems*, Vol. 4, No. 4, 1990, pp. 445–460.

[14]Goldberg, D. E., *Genetic Algorithms in Search, Optimization and Machine Learning*, Addison Wesley Longman, Reading, MA, 1989.